SUPPLEMENTARY TABLES AND FIGURES

Table S1.

Correlation between the relative decrease of Fv/Fm on the first day after increasing the growth irradiance from 100 µmol m^{-2} s^{-1} to 600 µmol m^{-2} s^{-1} (high light, HL) and other photosynthetic parameters during the acclimation period to increased growth irradiance

Table S2.

Annotations of the gene function as indicated in TAIR (www.arabidopsis.org) of all the genes found to be in linkage disequilibrium (r> 0.45) with the SNPS associated with a –log10(p) >4 for Φ_{PSII} measured one hour after a step-wise increase in irradiance from 100 to 550 µmol m^{-2} s^{-1}.

Figure S1.

Light response curves per accession in different constant growth irradiances

Figure S2.

Maximum relative electron transport rates (rETR) measured at saturating actinic irradiance per accession in different constant growth irradiances

Figure S3.

Variation in parameterized value of the relation of maximum rETR with growth irradiance

Figure S4.

Complete variation in light response curves of rETR of all 12 accessions grown in low growth irradiance level (LL), response to high growth irradiance level (HL), or grown in HL

Figure S5.

Phenotypic distribution of Φ_{PSII} one day before (A) and one hour after (B) an increase in growth irradiance from 100 µmol m^{-2} s^{-1} to 550 µmol m^{-2} s^{-1} for the 344 accessions used for the GWAS.

Table S1. Correlation between the relative decrease of Fv/Fm on the first day after increasing the growth irradiance from 100 µmol m^{-2} s^{-1} to 600 µmol m^{-2} s^{-1} and other photosynthetic parameters during the acclimation period to increased growth irradiance. Dark grey cells indicated with ** represent significant correlations at P=0.05; light grey cells indicated with * represent significant correlations at P=0.10.

DAY0		F_v/F_m	F_v'/F_m'(600)	NPQ(600)	$_{qP}$(600)	Φ_{PSII}(600)
Decrease in F_v/F_m on day 1 relative to day 0	Pearson Correlation	0.088	0.031	0.025	.395**	0.296*
	Sig. (2-tailed)	0.616	0.862	0.886	0.019	0.085
DAY1 (after HL increase)		F_v/F_m	F_v'/F_m'(600)	NPQ(600)	$_{qP}$(600)	Φ_{PSII}(600)
Decrease in F_v/F_m on day 1 relative to day 0	Pearson Correlation	.792**	.077	.364**	.525**	.393**
	Sig. (2-tailed)	.000	.659	.032	.001	.019
DAY2 (after HL increase)		F_v/F_m	F_v'/F_m'(600)	NPQ(600)	$_{qP}$(600)	Φ_{PSII}(600)
Decrease in F_v/F_m on day 1 relative to day 0	Pearson Correlation	.636**	.109	.255	.394**	0.286*
	Sig. (2-tailed)	.000	.533	.139	.019	.096
DAY3 (after HL increase)		F_v/F_m	F_v'/F_m'(600)	NPQ(600)	$_{qP}$(600)	Φ_{PSII}(600)
Decrease in F_v/F_m on day 1 relative to day 0	Pearson Correlation	.617**	0.311*	-.040	.387**	.396**
	Sig. (2-tailed)	.000	.069	.819	.022	.018
DAY4 (after HL increase)		F_v/F_m	F_v'/F_m'(600)	NPQ(600)	$_{qP}$(600)	Φ_{PSII}(600)
Decrease in F_v/F_m on day 1 relative to day 0	Pearson Correlation	.505**	0.306*	-.084	.382**	.365**
	Sig. (2-tailed)	.002	.074	.631	.024	.031

Table S2. Annotations of the gene function as indicated in TAIR (www.arabidopsis.org) of all the genes found to be in linkage disequilibrium (r> 0.45) with the SNPS associated with a –log10(p) >4 for Φ_{PSII} measured one hour after a step-wise increase in irradiance from 100 to 550 µmol m^{-2} s^{-1}.

Gene	Description
AT1G21060	Unknown protein
AT1G21065	Unknown protein
AT1G21070	Nucleotide-sugar transporter family protein
AT1G21100	IGMT1, indole glucosinolate O-methyltransferase 1
AT1G21110	IGMT3, indole glucosinolate O-methyltransferase 3
AT1G21120	IGMT2, indole glucosinolate O-methyltransferase 2
AT1G21130	IGMT4, indole glucosinolate O-methyltransferase 4
AT1G21140	Nodulin-like1, transcript abundance repressed under conditions of Fe-deficient growth
AT1G74190	Receptor-like protein 15, located in endomembrane system
AT2G26290	Root-specific kinase1
AT3G04880	Encodes a novel protein involved in DNA repair from UV damage
AT3G04890	Unknown protein
AT3G04900	Heavy metal transport/ detoxification superfamily protein
AT3G04903	Encodes a defensin-like family protein
AT3G05790	Lon-protease 4, for degradation of abnormal, damaged, and unstable protein
AT3G05800	AIF1 (activation-tagged BRI1 suppressor 1)-interacting factor 1, involved in MAPK cascade, major regulator
AT3G05810	Chromatin assembly/disassembly protein
AT3G05820	Encodes a putative plastid-targeted alkaline/neutral invertase
AT3G05830	Encodes an intermediate filament-liek protein, function unknown
AT3G05835	tRNA-Ile
AT3G05840	Encodes a kinase involved in meristem organization
AT3G05850	Encodes a member of a domesticated transposable element gene family
AT3G05858	Unknown protein
AT3G05870	Subunit of the anaphase promoting complex in cell division
AT3G05880	Encodes a small, highly hydrophobic protein induced by low temperatures, dehydration and salt stress (A)
AT3G05890	Encodes a small, highly hydrophobic protein induced by low temperatures, dehydration and salt stress (B)
AT3G54000	Unknown protein
AT4G21750	MERISTEM LAYER 1, a homeobox protein similar to GL2; expressed in both the apical and basal daughter cells of the zygote.
AT4G21770	Pseudouridine synthase, involved in RNA modification
AT5G03750	Unknown protein
AT5G64910	Unknown protein
AT5G64920	Encodes a RING-H2 protein, involved in ubiquitination
AT5G64930	Regulator of expression of pathogenesis-related genes. Participates in signal transduction pathways involved in plant defence.
AT5G64940	Oxidative stress-related ABC1-like protein (ATP-binding cassette)
AT5G64950	Mitochondrial transcription termination factor family protein
AT5G64970	Mitochondrial substrate carrier family protein
AT5G64990	RAB GTPase homolog, GTPase activity, located in mitochondrion
AT5G65020	Annexin 2, calcium binding protein

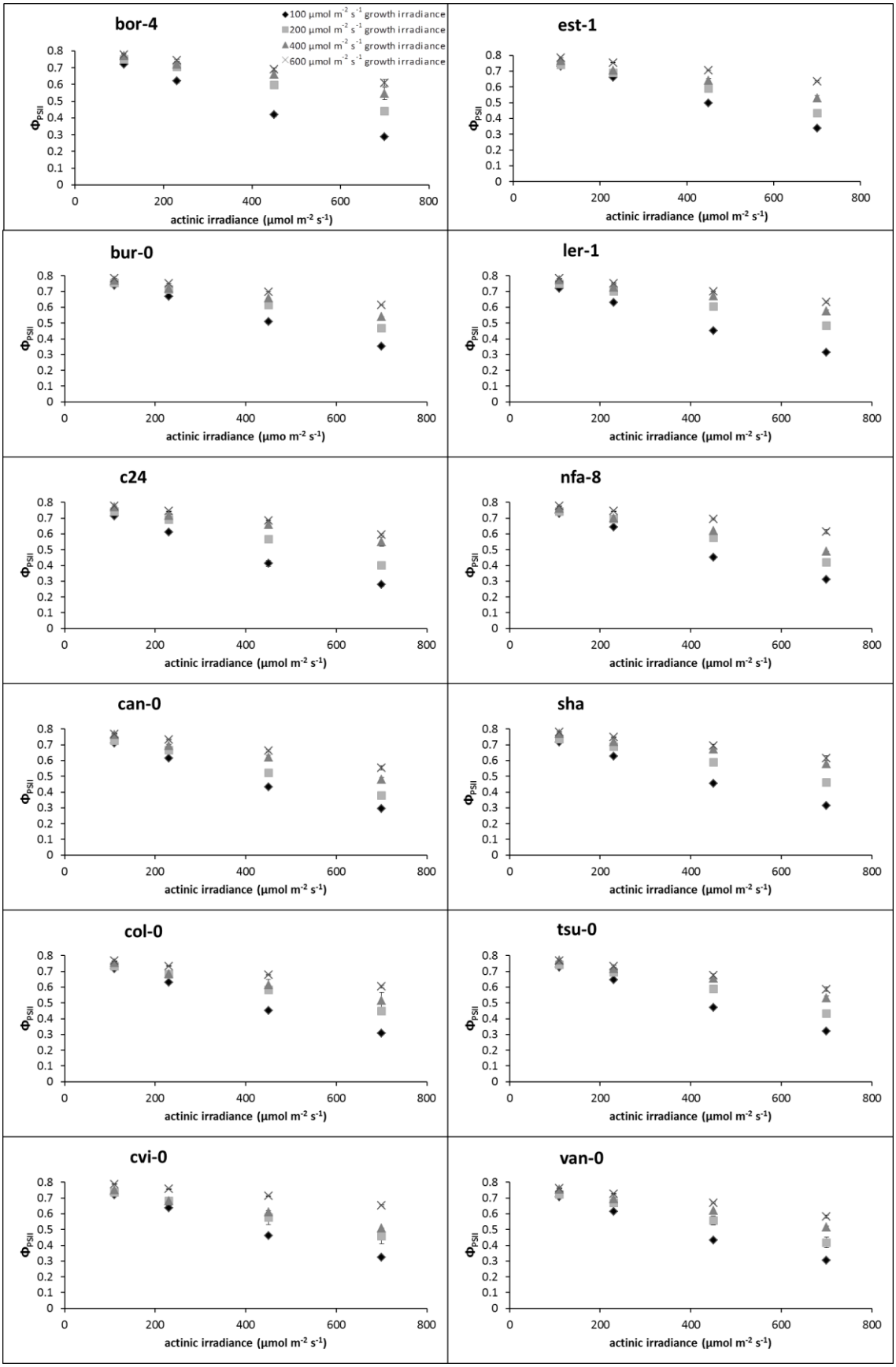

Figure S1. Light response curves per accession in different constant growth irradiances. Error bars indicate the standard error of the mean, N=3.

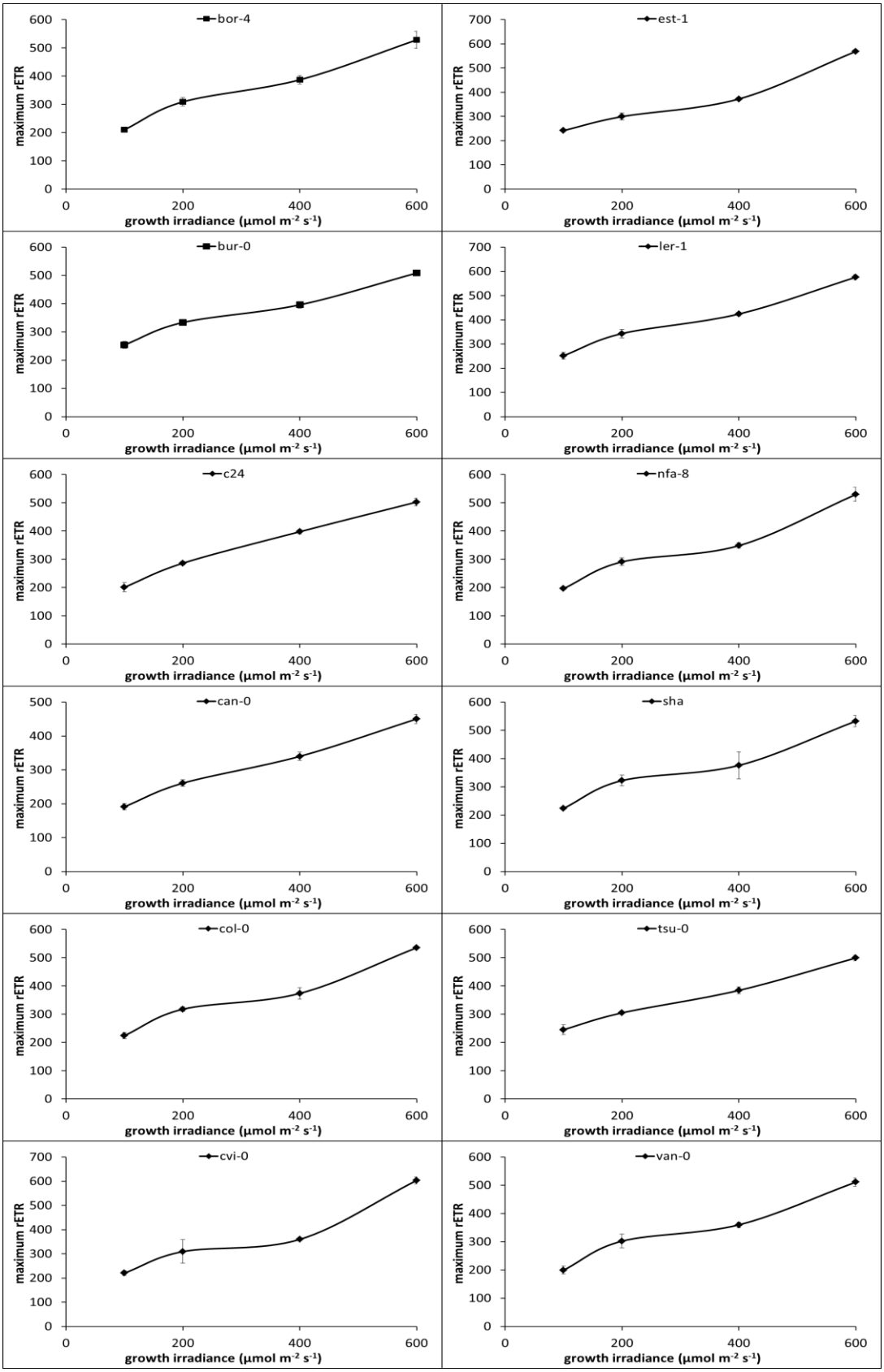

Figure S2. Maximum relative electron transport rates (rETR) measured at saturating actinic irradiance per accession in different constant growth irradiances. Error bars indicate the standard error of the mean, N=3.

A Descriptives					Tukey's HSD test		
					Subset for alpha = 0.05		
	N	Mean parameterized value	Std. Deviation	Std. Error	1	2	3
tsu-0	3	1.1117	.58950	.34035	1.1117		
c24	3	1.3907	.56734	.32755	1.3907	1.3907	
est-1	3	1.4367	.37650	.21737	1.4367	1.4367	
cvi-0	3	1.5407	.36650	.21160	1.5407	1.5407	1.5407
can-0	3	1.6290	.27900	.16108	1.6290	1.6290	1.6290
sha	3	2.1377	.12150	.07015	2.1377	2.1377	2.1377
bur-0	3	2.1720	.19300	.11143	2.1720	2.1720	2.1720
bor-4	3	2.3607	.98273	.56738	2.3607	2.3607	2.3607
col-0	3	2.5650	.63877	.36879	2.5650	2.5650	2.5650
ler-1	3	2.6727	.58750	.33919	2.6727	2.6727	2.6727
nfa-8	3	2.9483	.75612	.43655		2.9483	2.9483
van-0	3	3.1210	.52400	.30253			3.1210
Sig.					.067	.068	.061

47

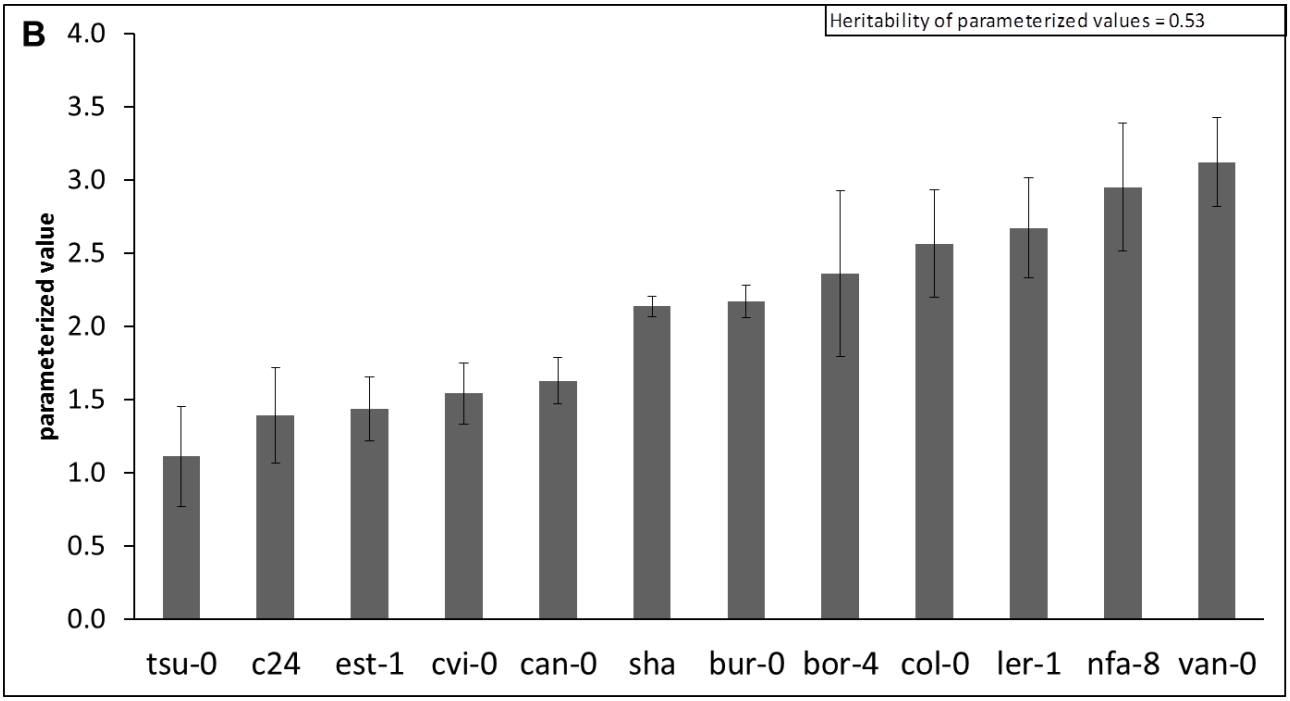

48

49 Figure S3. Variation in parameterized valueof the relation of maximum rETR with growth irradiance
50 level; (A) Descriptive ANOVA table including a Tukey's HSD test revealing three significantly
51 different groups for the parameterized value at p=0.05; (B) Variation in parameterized value for the
52 relation between photosynthetic capacity and growth irradiance, Error bars indicate the standard error
53 of the mean, N=3. The top right inset shows the heritability calculated for this trait.

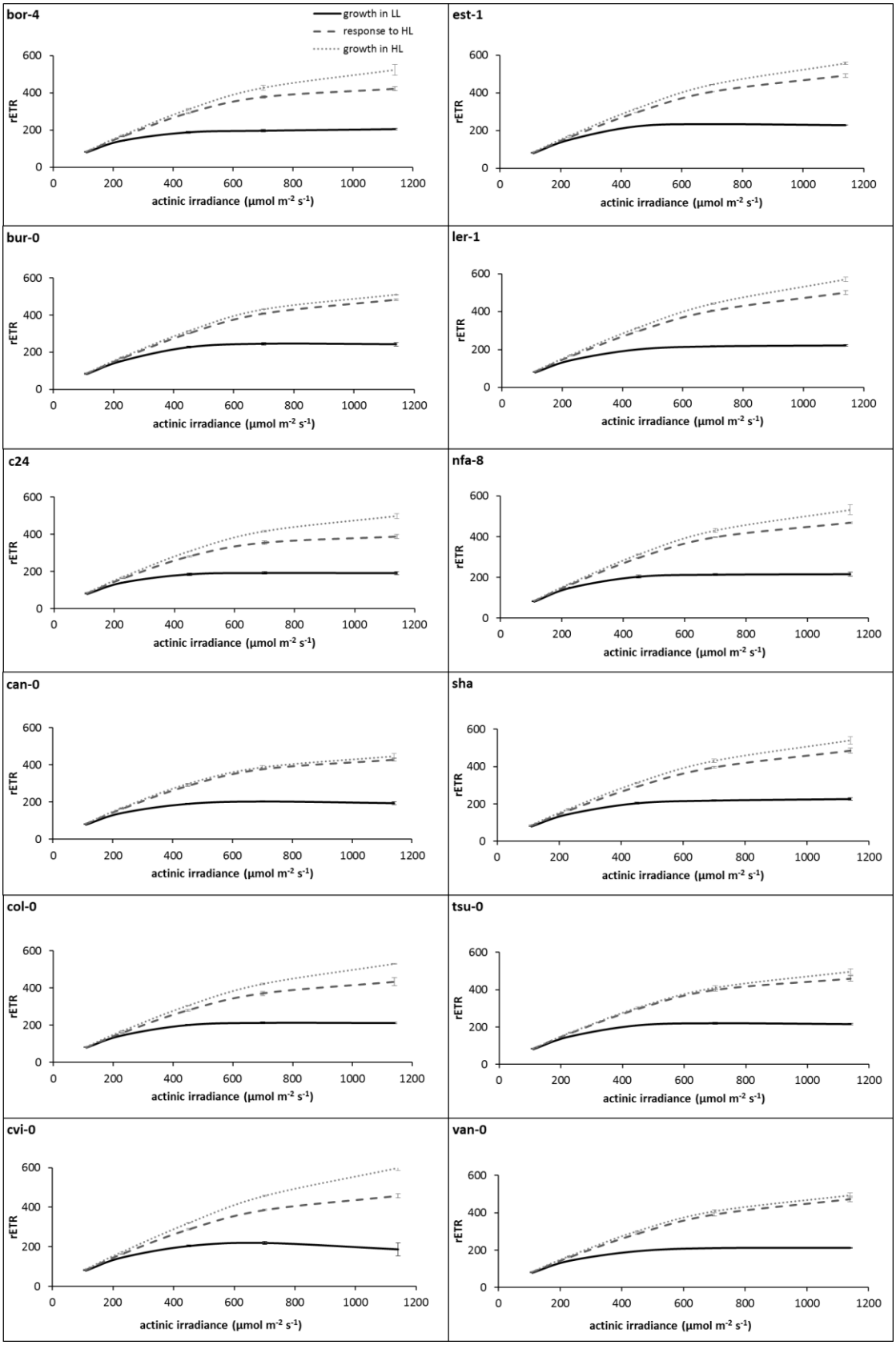

Figure S4. Complete variation in light response curves of rETR of all 12 accessions grown in low growth irradiance level (LL), response to high growth irradiance level (HL), or grown in HL

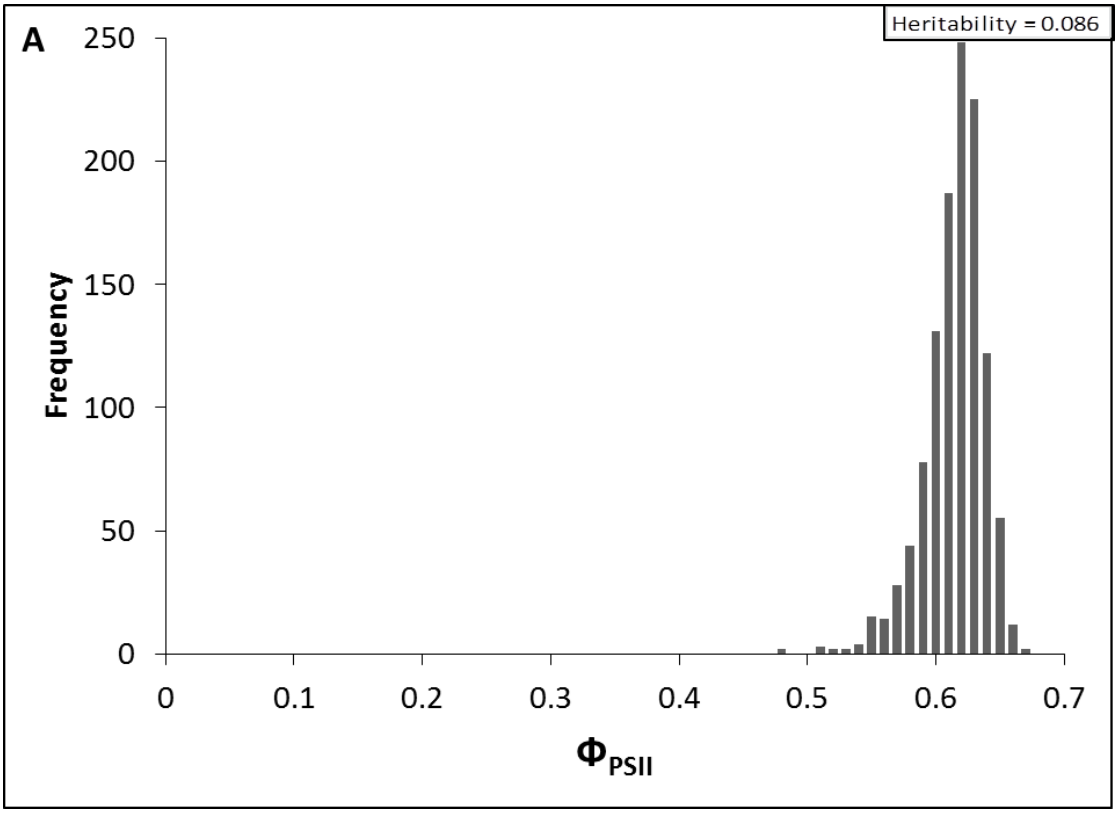

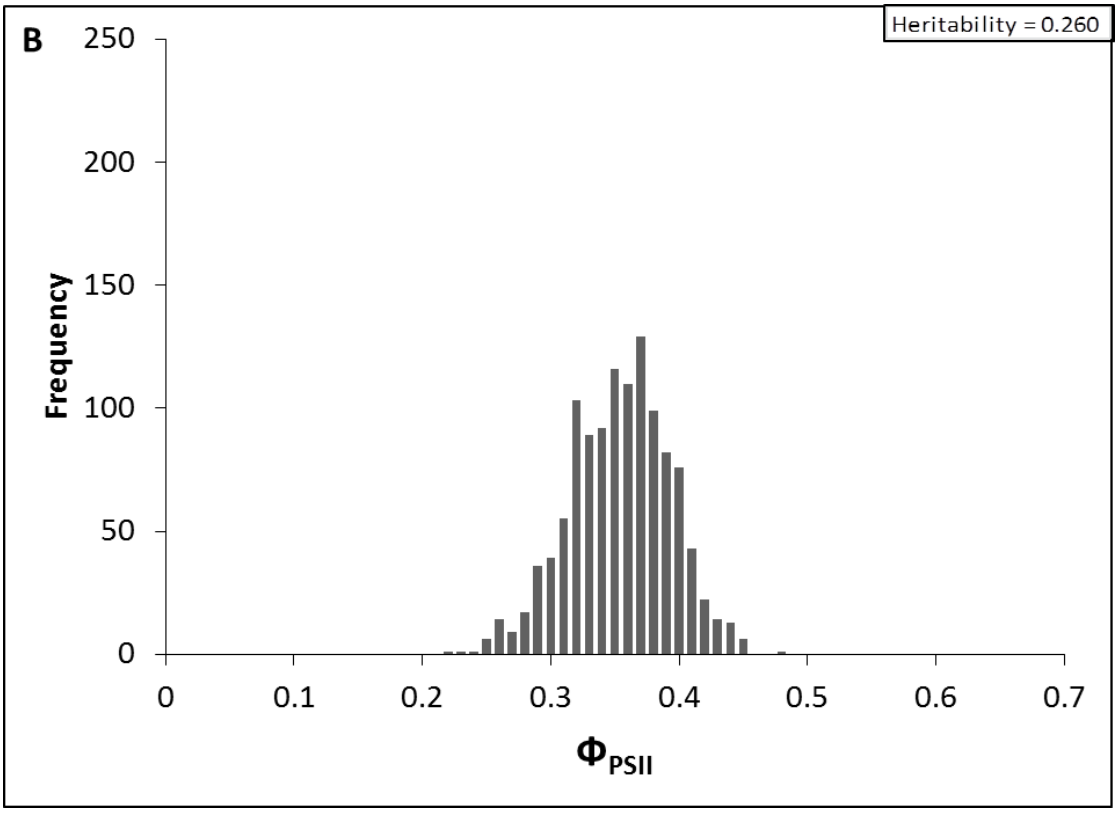

Figure S5. Phenotypic distribution of Φ_{PSII} one day before (A) and one hour after (B) an increase in growth irradiance from 100 µmol m^{-2} s^{-1} to 550 µmol m^{-2} s^{-1} for the 344 accessions used for the GWAS.